LA-5944-PR
Progress Report

Special Distribution
Issued: April 1975

Applied Nuclear Data Research and Development Quarterly Progress Report

October 1 through December 31, 1974

Edited by

G. M. Hale
D. R. Harris
R. E. MacFarlane

los alamos
scientific laboratory
of the University of California
LOS ALAMOS, NEW MEXICO 87544

An Affirmative Action/Equal Opportunity Employer

UNITED STATES
ENERGY RESEARCH AND DEVELOPMENT ADMINISTRATION
CONTRACT W-7405-ENG. 36

The four most recent reports in this series, unclassified, are:

LA-5570-PR	LA-5727-PR
LA-5655-PR	LA-5804-PR

In the interest of prompt distribution, this progress report was not edited by the Technical Information staff.

Work performed under the joint auspices of the U.S. Energy Research and Development Administration's Divisions of Military Application, Reactor Research and Development, and Controlled Thermonuclear Research, as well as the Defense Nuclear Agency of the Department of Defense, and the National Aeronautics and Space Administration.

CONTENTS

I. Nuclear Cross-Section Processing..... 1

II. Nuclear Data Processing for HTGR Safety Research..... 4

III. Nuclear Data for the Controlled Fusion Program..... 5

IV. Cross Sections for Radiotherapy Shield-Collimator Design.. 6

V. Sensitivity Theory and Sensitivity Profiles..... 6

VI. Techniques for Selecting Multigroup Structures..... 9

VII. Technique for Simultaneous Adjustment of Large Nuclear Data Libraries..... 11

VIII. Medium Energy Library..... 13

IX. ENDF/B-IV Yield, Decay, and Cross-Section Files..... 16

X. Absorption Library for Fission Products..... 16

XI. Gas Content in Irradiated Fuels..... 16

XII. CINDER Code..... 16

XIII. Gamma and Photoneutron Spectra..... 16

XIV. Study of the $T(d,n)^4He$ Cross Sections..... 17

XV. Neutron-Induced Gamma-Ray Production Cross Sections for Tungsten..... 17

XVI. A New n-d Evaluation for DNA..... 17

XVII. Proposed Format for Neutron Induced Radioactive Decay Data in ENDF/B..... 17

XVIII. Evaluations of Neutron-Induced Cross Sections of Li and ^{15}N..... 18

References..... 18

Items I, VI, VII, IX, X, XI, XII, XIII, XVII, and XVIII include work for DRRD. Items I, V, VIII, XIV, and XVIII include work for DMA. Items IX, XII, XV, and XVI include work for DNA. Items III and XIV include work for DCTR. Item VIII includes work for NASA. Item II includes work for DRSR.

APPLIED NUCLEAR DATA RESEARCH AND DEVELOPMENT

QUARTERLY PROGRESS REPORT

October 1 through December 31, 1974

Edited by

G. M. Hale, D. R. Harris, and R. E. MacFarlane

ABSTRACT

This report presents progress in provision of nuclear data for nuclear design applications. The work described here is carried out through the LASL Applied Nuclear Data Group and covers the period October 1 through December 31, 1974. The topical content of this report is summarized in the Contents.

I. NUCLEAR CROSS-SECTION PROCESSING (R. E. MacFarlane, R. B. Kidman, D. W. Muir, D. R. Harris, J. H. Hancock, and W. B. Wilson)

Group T-2 is supporting and developing a variety of computer codes for processing evaluated nuclear data into forms that can be used for design purposes. The group's capability includes multigroup neutron, gamma production, and gamma interaction cross sections; pointwise neutron and photon cross sections for continuous energy Monte Carlo codes; and a variety of data management, plotting, and format conversion functions. The following subsections summarize recent progress.

A. Cross Section Production (R. B. Kidman, R. E. MacFarlane, D. W. Muir, and W. B. Wilson

Extensive corrections to ENDF/B-IV were received from Brookhaven National Laboratory (BNL) this quarter, and they have been used to update our local set of ENDF/B-IV files. The revised files reside on PHOTOSTORE and are available to all Los Alamos Scientific Laboratory (LASL) users.

This data was used by MINX to produce a 50-group library in CCCC[1] format for 22 nuclides (see below).

Cross sections and reactor computing capabilities based on ETOX[2] and 1DX[3] were made available to LASL Group T-1 to enable them to perform scoping neutronic and safety calculations for the nuclear reactor Safety Test Facility. As the project progresses, more refined cross sections will be provided.

Pointwise cross sections in PENDF[4] format were produced for ^{235}U, ^{238}U, and ^{239}Pu from ENDF/B-IV for the LASL Theoretical Design division. These cross sections were generated at temperatures of 0, 300, 3 000, 30 000, 600 000, and 12 000 000 K using the advanced Doppler broadening capabilities of MINX described below.

Cross sections were also produced for ENDF/B-IV iron (MAT 1182) for use in the Radiotherapy Shield Design Project described in Section IV.

B. CCCC 50-Group, 22 Isotope Cross Section Library (R. B. Kidman and R. E. MacFarlane)

MINX has been used to generate a 50-group, 22-isotope, multigroup library from the updated ENDF/B-IV data. The isotopes chosen were those usually required in fast reactor calculations. Self-shielding factors were generated for three temperatures (300, 900, and 2 100 K) for all isotopes. The range of σ_0-values for each isotope was chosen to cover the element's most typical range of σ_0-values and to cover the element's probable range of f-factor variation. The current formats of the library are the CCCC ISOTXS and BROKXS files.[1]

The library will be used for Phase II Benchmark Testing of the ENDF/B-IV data. The library will also

be made available to off-site users so that we can begin to get feedback from outside use of MINX data.

Finally, five of the 22 isotopes (^{238}U, ^{239}Pu, ^{16}O, ^{23}Na, and Fe) were also generated in a 240-group structure (this is the CSEWG 239-group structure[5] with a thermal dump group added). This five isotope library will be used here and off site to discover any problems peculiar to this many-group library.

C. MINX Code Development (R. E. MacFarlane and R. B. Kidman)

During this quarter, extensive modifications were made to the routines which calculate transfer matrices for elastic and discrete inelastic scattering; these changes are discussed in more detail below. Extensive editing of the code was begun. This involves adding comment cards, removing unused variables and subroutines, cleaning up coding, and improving the format of the output listing. More of this editing will be done next quarter in preparation for releasing the MINX code. A number of minor problems were uncovered by comparison with ETOX[2] output and during the production of the 50-group library. These included an error in weighting the transport cross section, several errors in the CCCC output processor, problems with unresolved data with zero degrees of freedom for the gamma width together with a non-zero gamma width (for example, MAT 1264), and problems with discontinuities in the unresolved resonance parameters for the europium isotopes. In addition, a dump group was added to the standard CSEWG 239-group structure.[5]

D. Processing Code Validation (R. E. MacFarlane, R. B. Kidman, and D. R. Harris)

One of the most difficult and time-consuming parts of code development is validation. This applies to the "physics" codes (such as TWOTRAN and VENTURE) and to the interface system (CCCC) as well as to processing codes such as MINX. For this reason, the Division of Reactor Research and Development (DRRD) of the Atomic Energy Commission (AEC) has created a Code Evaluation Working Group (CEWG) to devise and carry out a program of checking the entire code system to be used in the design of commercial LMFBR's. Harris and MacFarlane attended the organizational meeting of the Working Group in Washington D. C. in October. MacFarlane was appointed Chairman of the Cross Section Processing Code Subcommittee. This Committee is charged with developing evaluation tools for the processing codes and with generating cross sections to be used by other sub-committees investigating the design codes.

Validation of the MINX code during this quarter consisted of comparing MINX cross sections and f-factors with those produced by ETOX. After an error in the transport cross section was corrected, the largest differences that could be found were a few percent. Extensive internal checks were carried out on the transfer matrix calculation in MINX as reported below. After extensive modifications, the code produced numbers which satisfied all sum rules and which were consistent for alternate calculational paths (i.e., CM or LAB calculation).

E. Doppler Broadening of Neutron Cross Sections to High Temperatures (J. H. Hancock, R. E. MacFarlane, and D. W. Muir)

In nuclear weapons, neutrons must propagate through materials at very high temperatures. The changes in cross sections caused by the thermal motions of the target nuclei are called "Doppler broadening" because the narrow resonance peaks in the reaction cross sections become broader. The original version of the processing code MINX did its Doppler broadening with the "kernel broadening" technique developed for the SIGMA1 code.[6] Unfortunately, this method ran into numerical difficulties for high temperatures and low neutron energies. The following discussion presents the modifications necessary to get correct answers for this interesting regime.

The effective cross section for temperature T is defined as that cross section which gives the same reaction rate for stationary target nuclei as the real cross section gives for the moving nuclei, or

$$\rho v \sigma_{eff}(T,v) = \iiint d^3v \rho |\vec{v} - \vec{v}'| \sigma(|\vec{v} - \vec{v}'|) P(\vec{v}',T) \quad (1)$$

where $\vec{v}$ is the velocity of the incident neutron, $\vec{v}'$ is the velocity of the target, ρ is the number density of the target nuclei, and $P(\vec{v}',T)$ describes the distribution of target velocities. In this form, σ_{eff} is just the cross section in the reference frame of the target; therefore, subsequent processing can use the familiar stationary target kinematics.

If the cross section is represented as a piecewise-linear function of energy, it is possible to express the effective cross section as a liner combination of the functions

$$H_n(a,b) = \frac{1}{\sqrt{\pi}} \int_a^b z^n e^{-z^2}\, dz \quad . \qquad (2)$$

In the original code, these integrals were computed as differences between the probability integrals

$$F_n(a) = \frac{1}{\sqrt{\pi}} \int_a^\infty z^n e^{-z^2}\, dz \quad . \qquad (3)$$

Here $F_0(a) = \frac{1}{2}\,\mathrm{erfc}(a)$ and the higher orders are easily generated by recursion. This is a simple and fast way to compute the $H_n(a,b)$, but it loses significance when a and b are small. For the new code, a method has been developed to compute $H_n(a,b)$ directly in this regime. This alternate method eliminates the numerical instabilities over the entire useful range. In fact, it gives reliable answers for $E = 10^{-5}$ eV and T = 1 keV where the original code returned negative cross sections.

To illustrate the behavior of the effective cross section at high temperatures, the new method was applied to two simple artificial isotopes. Figure 1 shows tedium-1 which has a constant scattering cross section of 1 barn, and Fig. 2 shows tedium-3 which has a single absorption resonance at 20 eV. In both cases, a stong 1/v tail appears at low energies.

This tail has been a surprise to most observers. It violates the intuitive feeling that the area under the cross section curve should remain constant. However, the basic definition of the effective cross section (see Eq. 1) preserves the reaction rate. For stationary targets, the reaction rate goes to zero as v goes to zero, but as the target nuclei begin to move, the reaction rate becomes non-zero even at v = 0. The only effective cross section which can give a non-zero reaction rate at v = 0 has a 1/v variation as observed in these two figures.

As a final example, Fig. 3 shows the total cross section for ^{238}U (ENDF/B-IV MAT 1262) at 30 000 and 12 000 000 K. The 1/v tails from the resonances in the resolved resonance region are apparent. Also note the dramatic smoothing of the function. These large effective cross sections at low energies will dramatically decrease the neutron flux in the range. This effect must be allowed for when producing group-averaged cross sections. However, the reduced number of neutrons in the low energy range also reduces the importance of the 1/v tail for many problems. Further study with appropriate test problems will be required to evaluate the importance of improved Doppler broadening at high temperatures.

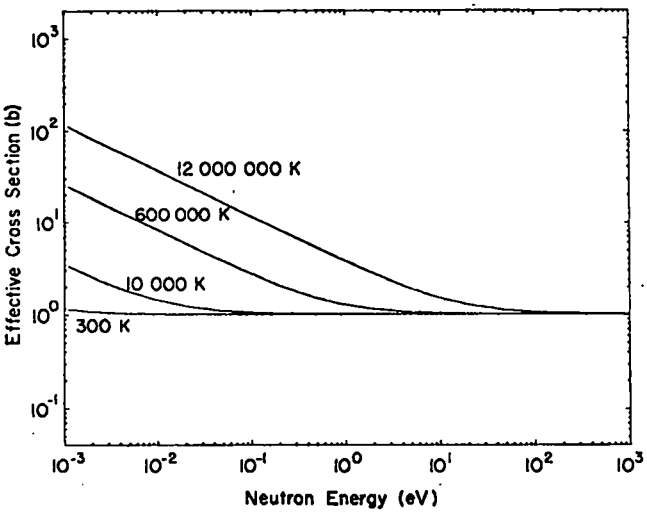

Fig. 1. Effective cross sections at 300, 10 000, 600 000, and 12 000 000 K for a nuclide with a constant actual cross section.

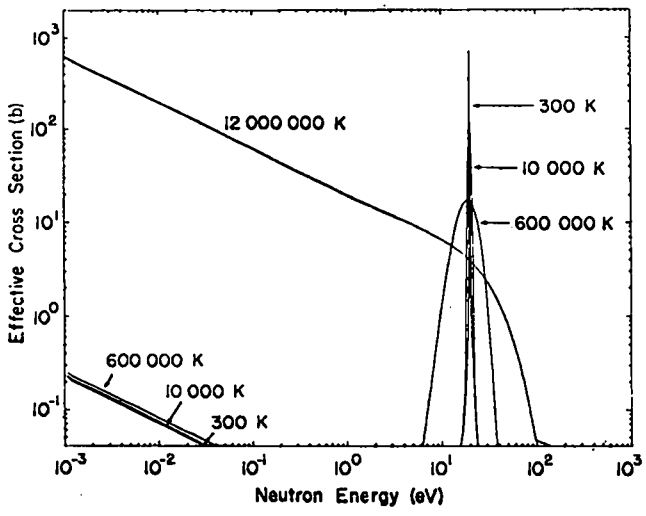

Fig. 2. Effective capture cross section at 300, 10 000, 600 000, and 12 000 000 K for a nuclide with a single S-wave resonance at 20 eV.

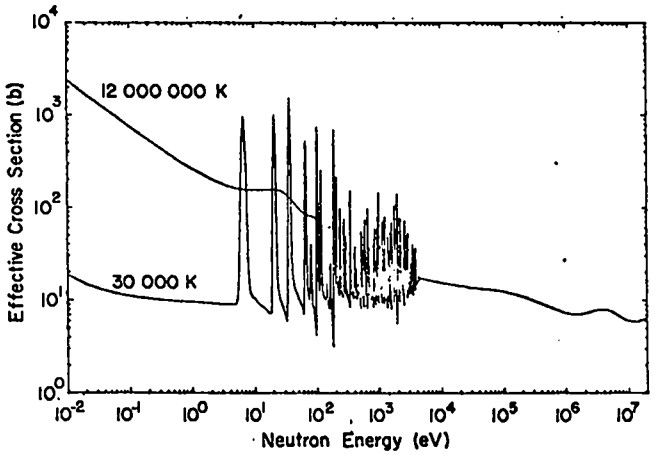

Fig. 3. Effective total cross section at 30 000 and 12 000 000 K for ^{238}U (ENDF/B-IV MAT 1262).

F. Calculation of Group Transfer Matrices in MINX (R. E. MacFarlane and W. B. Wilson)

The calculation of elements of the group-to-group transfer cross sections for discrete channel scattering is the single most time-consuming segment of the MINX code. In addition, the full and accurate treatment of anisotropy in scattering is one of the features of MINX which separates it from older processing codes. Therefore, special attention to the algorithms used for this calculation is warranted. During this quarter, extensive internal checks of the scattering matrices were carried out by (1) verifying sum rules, (2) checking convergence, and (3) comparing calculations done in the laboratory system with independent center-of-mass results. These experimental results were coupled with error analyses of both the LAB and CM calculations. Most of the tests were performed on ENDF/B-IV iron (MAT 1182).

The laboratory system calculation[7] was found to perform very well for low to moderate incident energies; in fact, it is exact as long as the number of Legendre terms required for the LAB expansion is not too large. However, the error analysis and test results show that this method becomes very inaccurate for small elastic removal cross sections at high incident energies. Although the exact result could theoretically be regained by using a very high order of Legendre expansion, in practice it becomes much more efficient to shift to a direct integration in the center-of-mass when the Legendre order of the LAB expansion exceeds 12 or 14. This mixed strategy together with some coding improvements discussed below decreased the time required to compute transfer matrices with MINX by factors of from 3 to 10.

In the course of this investigation, several errors and inefficiencies were discovered and corrected. This involved (1) a complete rewrite of the routine used for converting tabulated angular distributions to Legendre coefficients, (2) major changes to the routine used to determine the Legendre order of the LAB expansion needed to obtain the required accuracy, (3) changes to correct and improve the efficiency of the center-of-mass calculation, and (4) modifications needed to implement the mixed calculational strategy discussed above. In addition, this opportunity was used to clean-up and comment the coding in this part of MINX.

G. MINX-II Code Development (R. E. MacFarlane)

During this quarter, the extensions required to process the delayed neutron files from ENDF/B-IV were completed and tested. Some errors in the data files were discovered and reported to the National Neutron Cross Section Center (NNCSC) at Brookhaven National Laboratory (BNL). In addition, an output processor module was written to provide CCCC-III DLAYXS files from the delayed neutron data. These files will be used by LASL Group T-1 in the LMFBR Safety Program.

II. NUCLEAR DATA PROCESSING FOR HTGR SAFETY RESEARCH (M. G. Stamatelatos and R. J. LaBauve)

Various possible routes for generating multigroup cross sections for HTGR neutronic calculations in the thermal region were described in previous progress reports. Future plans indicate use of the LASL code system MINX.[8]

The present route for generating multigroup cross sections for comparison with cross sections generated outside LASL (e.g., Gulf General Atomic) at all necessary temperatures is shown in Fig. 4.

MC^2 is being used for generating above-thermal fine-group cross sections and for calculating an above-thermal neutron spectrum to be further used for collapsing the fine-group set to a broad-group set.

In the thermal region, the MC^2 code is being used for calculating fine-group absorber cross sec-

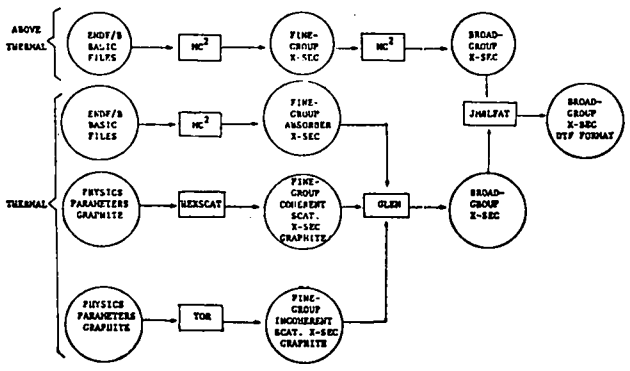

Fig. 4. Data flow for HTGR cross-section generation.

tions. The fine-group moderator (i.e., graphite) scattering cross sections are generated from physics parameters (e.g., Bragg edges, phonon distribution, etc.) by use of the HEXSCAT[9] code and of the LASL code TOR.[10] HEXSCAT calculates coherent scattering cross sections in hexagonal lattices and TOR calculates the scattering cross sections in the incoherent approximation. The direct use of these codes rather than the processing of the graphite ENDF thermal files by codes like FLANGE[11] is motivated by the fact that the data on these files are currently incomplete for the required energy range and must be complemented by additional calculations. Also, the energy grid for which the available graphite thermal data are tabulated on ENDF files does not necessarily correspond to the fine energy grid used and, if used, the data on these files require interpolation.

The fine-group thermal cross sections are used by the GLEN[12] code to calculate a thermal neutron spectrum which is further used to collapse the fine-group cross sections to the desired broad-group set.

The above-thermal and the thermal broad-group cross sections are then merged and formatted for use in the DTF[13] code by JMBLFAT.[14]

III. NUCLEAR DATA FOR THE CONTROLLED FUSION PROGRAM (D. W. Muir, L. Stewart, G. M. Hale, and D. R. Harris)

The CTR nuclear data program concentrated in this quarter on the assessment of near-term nuclear data needs. In addition, cross-section support was provided to the LASL insulator research program.

In order to coordinate our data assessment effort with programs at other laboratories, active participation has been maintained in the CTR subcommittee of the U. S. Nuclear Data Committee, in the ASTM Neutron Dosimetry Standards Committee, and in the Cross Section Evaluation Working Group. The reaction cross sections for the D-T and T-T fusion reactions have also been reviewed for incident-particle energies below 1 MeV.[15] Discrepancies as large as a factor of two in the T-T data and up to 15% in the D-T data were noted. Also, input was provided to the national nuclear data request list for new cross-section measurements and evaluations required for CTR applications, and requests from other laboratories were reviewed.

Work has begun on a program to determine quantitatively the cross-section requirements and highest priority areas for near-term nuclear data research and development for the national CTR program. This assessment takes into account the quality of currently available data, the sensitivity of important nuclear design parameters to data uncertainties, and the accuracy required in CTR design applications. These analyses use forward and adjoint transport calculations to calculate sensitivities and covariance matrices constructed from ENDF/B error files or other sources. A short program COVAR has been written to construct covariance matrices using the "range-parameter" formalism.[16]

In order to calculate sensitivity coefficients for secondary energy distributions, we have developed an extension of the usual perturbation approach. The main feature of this method is the introduction of a "sub-partial" reaction cross section $\hat{\sigma}$, which corresponds to just those events yielding high-energy secondary neutrons.[17] The sensitivity coefficient for $\hat{\sigma}$ is calculated by an algorithm which allows one to separate the effect of uncertainty in the spectrum from uncertainty in the energy-integrated cross-section magnitude. One important application of this method is to provide a quantitative basis for the assignment of priorities to measurements of neutron emission spectra. Such measurements were requested for a number of light elements in the CTR cross-section request list mentioned above.

Spectrum-averaged transmutation cross sections have been calculated for Be, N, O, Al, and Si using the data in the multigroup library described in Ref. 18. The energy spectrum used in the averaging is that calculated in the first wall of the RTPR. These data make possible predictions of the build-up of gaseous and metallic impurities in insulating materi-

als such as BeO, Si_3N_4, SiO_2, AlN, and Al_2O_3. In addition, we have reviewed the available experimental data for nuclear reactions between high-energy protons and various insulator materials in support of radiation damage experiments using proton-simulation techniques.

IV. CROSS SECTIONS FOR RADIOTHERAPY SHIELD-COLLIMATOR DESIGN (W. B. Wilson and D. R. Harris)

The code DANA5 has been used to produce P-5, 121-group iron cross sections for neutrons in the energy range 1.39×10^{-4} eV - 6.0×10^{7} eV. The lower 102 energy groups below 20 MeV were processed from ENDF/B-IV MAT 1192 by MINX. The upper 19 medium energy group cross sections were added by DANA5 by processing the point energy non-elastic cross-section results of the internuclear cascade and evaporation code CROIX.

A second cross-section set including elastic scattering above 20 MeV was also produced. Elastic scattering is not included in the physics of CROIX, so the required elastic scattering cross-section data were computed using the optical model code ABACUS and processed by MINX.[19] An attempt to apply a modified diffraction theory for this purpose was abandoned due to poor agreement with experimentally measured angular distributions at back angles.

The cross-section sets with and without elastic scattering are used in evaluating the significance of including elastic scattering above 20 MeV in low-medium energy transport calculation in iron. The complete set is used in determining cross-section sensitivities in the development of a cross-section set with fewer groups to be used in the design of the TAMVEC radiotherapy shield collimator unit.[20]

V. SENSITIVITY THEORY AND SENSITIVITY PROFILES (D. R. Harris, W. B. Wilson, and M. G. Stamatelatos)

Nuclear data sensitivity theory, which has been described previously by numerous authors, is here reexamined so as (1) to be general and compact, and (2) to redevelop and expand the Bartine et al.[21,22] concept of a sensitivity profile in a context required for the next section (Technique for Selecting Multigroup Structure). The development arrives at only one of the two Bartine et al. alternative definitions of sensitivity profile, and we show by means of a soluble analytic case that the alternative definitions are not generally equivalent.

The particle or photon flux $\psi(\xi)$ at a point ξ in phase-time space satisfies the linear Boltzmann equation

$$L\psi = S \quad , \tag{4}$$

where $S(\xi)$ is the local source strength. The adjoint flux $\psi^+(\xi)$ satisfies the adjoint equation

$$L^+\psi^+ = S^+ \quad , \tag{5}$$

where $S^+(\xi)$ is an adjoint source, and where L^+ is an operator adjoint to the Boltzmann operator L. The adjoint operator and boundary conditions on ψ^+ are defined such that

$$(\psi^+, L\psi) = (L^+\psi^+, \psi) \quad , \tag{6}$$

where (ϕ,χ) is an inner product, in this case just the integral of $\phi(\xi)\,\chi(\xi)$ over the relevant region of phase-time space.

Choose $S^+(\xi)$ so that (S^+,ψ) is an integral quantity of interest. Suppose that the operators and sources change as, for example, might occur if nuclear data are changed. Then

$$(L + \delta L)(\psi + \delta\psi) = S + \delta S \quad , \tag{7}$$

$$(L^+ + \delta L^+)(\psi^+ + \delta\psi^+) = S^+ + \delta S^+ \quad . \tag{8}$$

Combining the previous equations, it follows that the exact change $\delta(S^+,\psi)$ in the integral quantity, even for large changes in operators and sources, is

$$\delta(S^+,\psi) = -(\psi^+, \delta L[\psi + \delta\psi]) + (\psi^+, \delta S) + (\delta S^+, \psi + \delta\psi) \quad , \tag{9}$$

or

$$\delta(S^+,\psi) = -(\delta L^+[\psi^+ + \delta\psi^+], \psi) + (\psi^+ + \delta\psi^+, \delta S) + (\delta S^+, \psi) \quad , \tag{10}$$

as well as two other equivalent forms.

Hitherto we have been completely general, but from now on we confine ourselves to the case of fixed source and small perturbations. In this case,

$$\delta(S^+,\psi) = -(\psi^+, \delta L\psi) = (-\delta L^+\psi^+, \psi) \quad . \tag{11}$$

Further consider the time-independent, one-space dimensional, multigroup situation for which the

Boltzmann equation and its adjoint are

$$(\underline{\Omega}\cdot\nabla + \Sigma_g)\psi_g(\underline{r},\underline{\Omega})$$

$$- \sum_{g'}\sum_{j=0}^{\infty} \frac{2j+1}{4\pi} \Sigma^j_{g'\to g}\psi_{g'j}(\underline{r})P_j(\mu) =$$

$$= S_g(\underline{r},\underline{\Omega}) \qquad (12)$$

and

$$(-\underline{\Omega}\cdot\nabla + \Sigma_g)\psi^+_g(\underline{r},\underline{\Omega})$$

$$- \sum_{g'}\sum_{j=0}^{\infty} \frac{2j+1}{4\pi} \Sigma_{g\to g'}\psi^+_{g'j}(\underline{r})P_j(\Omega)$$

$$= S^+_g(\underline{r},\underline{\Omega}) \quad . \qquad (13)$$

Here $\psi_g(\underline{r},\underline{\Omega})$ and $\psi^+_g(\underline{r},\underline{\Omega})$ are the flux and adjoint flux, respectively, at position $\underline{r}$, in multigroup g, and in direction $\underline{\Omega}$, with Legendre expansions

$$\psi_g(\underline{r},\underline{\Omega}) = \sum_{j=0}^{\infty} \frac{2j+1}{4\pi} \psi_{gj}(\underline{r})P_j(\mu) \quad , \qquad (14)$$

$$\psi^+_g(\underline{r},\underline{\Omega}) = \sum_{j=0}^{\infty} \frac{2j+1}{4\pi} \psi^+_{gj}(\underline{r})P_j(\mu) \quad , \qquad (15)$$

in terms of the Legendre polynomials, $P_j(\mu)$, of the polar angle cosine μ. The Legendre coefficients of flux, ψ_{gj}, and adjoint flux, ψ^+_{gj}, are readily computed from S_N, multigroup Monte Carlo, P_N, and diffusion theory solutions, and their use eliminates the necessity for determining consistent quadrature techniques for the inner product, so we utilize Legendre fluxes and adjoint fluxes henceforth. In this case, the inner product expressions of Eq. (11) become

$$\delta(S^+,\psi) = -(\psi^+,\delta L\psi) = \int d\underline{r} \sum_g \sum_{j=0}^{\infty} \frac{2j+1}{4\pi} \psi^+_{gj}$$

$$\left[-\delta\Sigma_g\psi_{gj} + \sum_{g'}\delta\Sigma^j_{g'\to g}\psi_{g'j}\right] \quad , \qquad (16)$$

and

$$\delta(S^+,\psi) = -(\delta L^+\psi^+,\psi) = \int d\underline{r} \sum_g \sum_{j=0}^{\infty} \frac{2j+1}{4\pi}$$

$$\left[-\delta\Sigma_g\psi^+_{gj} + \sum_{g'}\delta\Sigma^j_{g\to g'}\psi^+_{g'j}\right]\psi_{gj} \quad , \qquad (17)$$

for the change in the integral quantity consequent to changes in group cross sections. Thus for changes in particular cross sections, we obtain from either Eq. (16) or (17) the results

$$\frac{\partial(S^+,\psi)}{\partial\Sigma_g} = -\int d\underline{r} \sum_{j=0}^{\infty} \frac{2j+1}{4\pi} \psi^+_{gj}\psi_{gj} \quad , \qquad (18)$$

$$\frac{\partial(S^+,\psi)}{\partial\Sigma^j_{g\to g}} = \int d\underline{r} \sum_{j=0}^{\infty} \frac{2j+1}{4\pi} \psi^+_{gj}\psi_{g'j} \quad . \qquad (19)$$

These derivatives, which are computed in the ALVIN code by a subroutine SENSI from fluxes and adjoints read by subroutine READFLUX, completely characterize cross-section sensitivities. There are so many of the derivatives

$$\partial(S^+,\psi)/\partial\Sigma^j_{g'\to g} \quad ,$$

however, that it is useful to condense them into a group dependent quantity, the sensitivity profile, P_g, introduced by Bartine et al.[21,22] Suppose that for cross sections of a particular type or nuclide x the total cross section in group g changes, and that the group-to-group transfer cross sections change accordingly, so that

$$\frac{\delta\Sigma^{jx}_{g\to g'}}{\Sigma^{jx}_{g\to g'}} = \frac{\delta\Sigma^x_g}{\Sigma^x_g} \qquad (20)$$

for all exit groups g' and Legendre orders j. Cross sections for transferring particles into group g are unchanged, i.e.,

$$\frac{\delta\Sigma^{jx}_{g'\to g}}{\Sigma^{jx}_{g'\to g}} = 0, \; g' \neq g \quad . \qquad (21)$$

Then, compounding changes by the usual method

$$\delta y = \sum_i \frac{\partial y}{\partial x_i} \delta x_i$$

we have, from Eqs. (18-21)

$$\delta(S^+,\psi) = \frac{\delta(S^+,\psi)}{\partial \Sigma_g^x} \delta\Sigma_g^x + \sum_{g'} \sum_{j=0}^{\infty} \frac{\partial(S^+,\psi)}{\partial \Sigma_{g\to g'}^{jx}} \delta\Sigma_{g\to g'}^{jx},$$

$$= P_{gx} \frac{\delta\Sigma_g^x}{\Sigma_g^x} \quad , \tag{22}$$

where the sensitivity profile is defined as

$$P_{gx} = \int d\underline{r} \sum_{j=0}^{\infty} \frac{2j+1}{4\pi} \left[-\Sigma_g^x \psi_{gj}^+ + \sum_{g'} \Sigma_{g\to g'}^{jx} \psi_{g'j}^+ \right] \psi_{gj} \quad . \tag{23}$$

When the assumption Eq. 20 is unwarranted as, for example, when neutron emission spectra are changed, then Eq. (19) is relevant, and Eq. (22) and the sensitivity profile are not.

Bartine et al.[21] utilize this definition, Eq. (23), for sensitivity profile, but they appear to state, on the basis of Eqs. (6) and (11) that another definition can be used

$$P'_g = \int d\underline{r} \sum_{j=0}^{\infty} \frac{2j+1}{4\pi} \psi_{gj}^+ \left[-\Sigma_g^x \psi_{gj} + \sum_{g'} \Sigma_{g'\to g}^{jx} \psi_{g'j} \right] \tag{24}$$

In paraphrase, because $(\psi^+, \delta L\psi)$ equals $(\delta L^+\psi^+, \psi)$ then $\psi^+\delta L\psi$ equals $\psi\delta L^+\psi^+$ at each point in phase-time space. There appears to be no a priori reason to expect this to be true, although it is true for the fully absorptive case. We now provide the solution to an analytic case that is useful in understanding this and other problems, and for which P'_g does not equal P_g.

The Boltzmann equation for hydrogenous moderation without leakage is, expressed analogously to Eq. (4),

$$\Sigma(E)\psi(E) - \int_0^{\infty} dE' \Sigma_s(E') \frac{U(E'-E)}{E'} \psi(E') = S(E) \quad , \tag{25}$$

where U(E'-E) is unity if $E' \geq E$ and is zero otherwise. The adjoint equation is

$$\Sigma(E)\psi^+(E) - \int_0^{\infty} dE' \Sigma_s(E) \frac{U(E-E')}{E} \psi^+(E') = S^+(E) \quad , \tag{26}$$

and the adjoint operator L^+ obeys Eq. (6) for any boundary conditions $\psi(0)$, $\psi(\infty)$, $\psi^+(0)$, $\psi^+(\infty)$. The solution to Eq. (25) is well-known,

$$\psi(E) = \frac{S(E)}{\Sigma(E)} + \int_0^{\infty} dE'' \frac{S(E'')}{\Sigma(E)} \frac{C(E'')}{E''} e^{\int_E^{E''} dE' \frac{C(E')}{E'}} \quad , \tag{27}$$

in terms of the number of secondaries per collision $C(E) = \Sigma_s(E)/\Sigma(E)$.

The adjoint equation, Eq. (26), can be solved by transforming it into a differential equation

$$\frac{d\psi^+(E)}{dE} - a(E)\psi^+(E) = b(E) \tag{28}$$

where

$$a(E) = \frac{C(E)}{E} + \frac{d\ell n[C(E)/E]}{dE} \tag{29}$$

and

$$b(E) = \frac{d}{dE}\left[\frac{S^+(E)}{\Sigma(E)}\right] + \frac{S^+(E)}{\Sigma(E)} \frac{d[\ell nC(E)/E]}{dE} \tag{30}$$

The solution is

$$\psi^+(E) = \psi^+(0) e^{\int_0^E dE' a(E')} + \int_0^E dE'' b(E'') e^{\int_{E''}^E dE' a(E')} \tag{31}$$

for any dependence of C(E), $S^+(E)$ and $\Sigma(E)$ on energy.

We now turn to the sensitivity profiles P and P' defined in Eqs. (23) and (24). In the present case these are

$$P(E) = -\psi(E)L^+\psi^+(E) = -\psi(E)S^+(E), \quad , \tag{32}$$

and

$$P'(E) = -\psi^+(E)L\psi(E) = -\psi^+(E)S(E) \quad . \tag{33}$$

Inserting the solutions for $\psi(E)$ and $\psi^+(E)$ from Eqs. (27) and (31) one obtains quite different dependence of P(E) and P'(E) on energy. It is instructive to illustrate this by a simple case. Suppose

$$C(E) = C_0 E \quad , \tag{34}$$

$$S(E) = s \text{ for } E \leq \hat{E}, \; S(E) = 0 \text{ for } E > \hat{E} \quad , \tag{35}$$

$$S^+(E) = gE\Sigma(E) \quad . \tag{36}$$

Then

$$P(E) = -gsEe^{C_0(\hat{E} - E)} \tag{37}$$

and

$$P'(E) = -s\left\{\left[\psi^+(0) + \frac{g}{C_0}\right]e^{C_0E} - \frac{g}{C_0}\right\}. \tag{38}$$

These solutions are shown in Fig. 5 for choices of $\psi^+(0) = g/C_{0x}$ and $C_0E = 1$. The cross section $\Sigma(E)$ can have any variation, resonant or otherwise. It can be seen that the proper definition P(E) has the shape intuitively expected of a sensitivity profile for this case, while the questionable definiton P'(E) does not.

VI. TECHNIQUES FOR SELECTING MULTIGROUP STRUCTURES (D. R. Harris and W. B. Wilson)

Multigroup structures used in nuclear design have been selected in a variety of ways. The energy range of interest, e.g., 0-20 MeV for fission and fusion systems, is selected first. Then an upper limit, $\hat{N}$, on the number of energy groups is selected on the basis of permissible computer storage and running time for nuclear design codes. The actual number of energy groups, N, usually is set equal to $\hat{N}$ because it is thought, possibly erroneously, that computational accuracy thereby will be improved. Finally, the multigroup lower and upper boundaries, $E\check{g}$ and $E\hat{g}$, respectively, may be set for each of the N groups (g = 1, 2, ..., N) so as to produce roughly equal integrated group fluxes, ψc_{g0}, in each group, or to provide computational detail over some cross-section feature, or by some other technique.

Once multigroup structure has been set the nuclear design organization usually persists in use of this structure and, in fact, builds up more and more data in this format and more and more experience of the errors to be expected from its use. Nevertheless, there is economic incentive to develop improved multigroup structures for classes of nuclear design problems.

Weisbin and LaBauve[5] state that "the fundamental consideration...is that group constants are relatively insensitive to reasonable choices of the within-group weighting spectra." These authors were willing to increase the number of groups, N, until their objective was attained, but when, as in the nuclear design situation, N is set by economics, we suggest a different but analogous requirement:

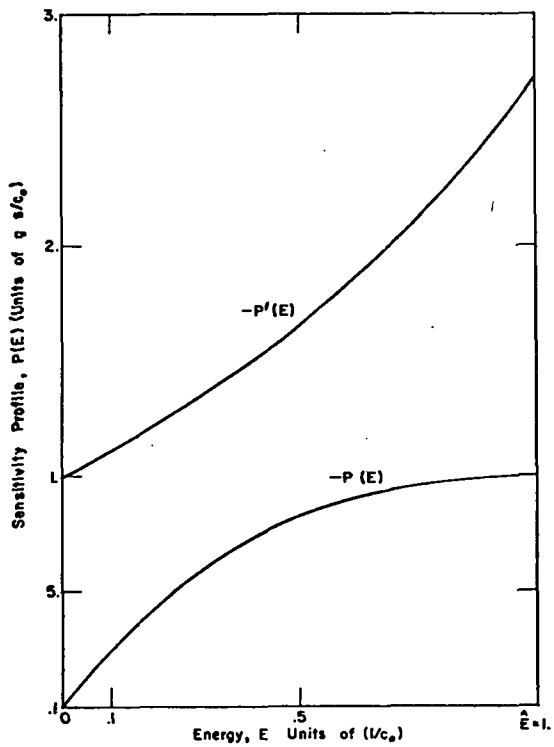

Fig. 5. Sensitivity profile, $P(\xi)$, and inappropriate definition P'(E), for hydrogenous moderation.

A. Select the design multigroup structure of N groups so that the relative errors in group constants resulting from reasonable alternative choices of the within-group spectra are roughly constant from group to group; thus the worst relative error is brought down near the average error.

But this cannot be the whole story, because errors in group constants for some groups are not as important as those for other groups. Oblow[23] has proposed that the design multigroup structure should be set by requiring the sensitivity profile (see previous section) computed for a much finer multigroup structure and integrated over each of the design multigroups be the same for each design multigroup. We suggest a somewhat different but analogous expression of Oblow's recommendation:

B. Select the design multigroup structure of N groups so that the sensitivity profile, P_g, defined in Eq. (23) of the previous section, is independent of multigroup g.

Requirements A and B can lead to very different choices of multigroup structures.

We now show that A and B imply each other and should be applied together, although even more general techniques emerge. If the within-group weighting spectra were correctly chosen at each point of phase space, then any multigroup structure (even one group) could be satisfactory. In fact, however, a set of within-group weighting spectra may be selected and applied to space-time points and physical situations where the spectra will be inappropriate. Consider a set of $\hat{1}$ alternative reasonable within-group weighting spectra $w_g^{(1)}(E)$, $w_b^{(2)}(E)$, ..., $w_g^{(\hat{1})}(E)$. For each of these $w_g^{(i)}(E)$ for group g we compute a group total macroscopic cross section $\Sigma_g^{(i)}$ and a set of group-to-group transfer cross sections $\Sigma_{g\,g'}^{j(i)}$. There will be a mean cross section

$$\langle \Sigma_g \rangle = \frac{1}{\hat{1}} \sum_{i=1}^{\hat{1}} \Sigma_g^{(i)} \quad , \tag{39}$$

a deviation from the mean for each choice,

$$\delta\Sigma_g^{(i)} = \Sigma_g^{(i)} - \bar{\Sigma}_g \quad , \tag{40}$$

so that the expected value vanishes

$$\langle \delta\Sigma_g \rangle = 0 \quad , \tag{41}$$

and a secondary moment measure of the uncertainty of dispersion of the error

$$\langle (\delta\Sigma_g)^2 \rangle = \frac{1}{\hat{1}} \sum_{i=1}^{i} (\delta\Sigma_g^{(i)} - \langle \delta\Sigma_g \rangle)^2 \quad . \tag{42}$$

Now consider an integral nuclear design quantity, (S^+,ψ), as introduced in the previous section. The change in the integral quantity resulting from a change in group cross sections can be determined from the general Eqs. (18) and (19) of the previous section. If we assume, however, that the changes in group-to-group transfer cross sections resulting from a change in weight function used in group g satisfy Eqs. (20) and (21) of the previous section, i.e.,

$$\frac{\delta\Sigma^j_{g\to g'}}{\bar{\Sigma}^j_{g\to g'}} = \frac{\delta\Sigma_g}{\bar{\Sigma}_g} \quad , \tag{43}$$

for all g' and j, and

$$\frac{\delta\Sigma^j_{g'\to g}}{\bar{\Sigma}^j_{g'\to g}} = 0, \; g' \neq g \quad , \tag{44}$$

then from Eq. (22) of the previous section

$$\delta(S^+,\psi) = P_g \frac{\delta\Sigma_g}{\Sigma_g} \quad . \tag{45}$$

The expected value of this change is zero, by Eq. (41), but its mean-square error is not,

$$\langle [\delta(S^+,\psi)]^2 \rangle = \sum_g \sum_{g'} P_g P_{g'} \left\langle \frac{\delta\Sigma_g \, \delta\Sigma_{g'}}{\bar{\Sigma}_g \, \bar{\Sigma}_{g'}} \right\rangle \quad . \tag{46}$$

Suppose there is a cross-section feature, e.g., a resonance or window, at the boundary between two adjacent groups. Then a shift in weighting function in each group from $1/E$ to $1/E^2$ illustrates that correlations are to be expected between group cross sections. For simplicity, however, suppose that $\delta\Sigma_g$ and $\delta\Sigma_{g'}$ are uncorrelated or are weakly correlated. Then

$$\langle [\delta(S^+,\psi)]^2 \rangle = \sum_g P_g^2 \left\langle \left[\frac{\delta\Sigma_g}{\bar{\Sigma}_g} \right]^2 \right\rangle \quad . \tag{47}$$

We wish to minimize this error.

Nature presents us with a certain set of cross-section features for all the nuclides likely to be in the class of problems of interest. If, given the requirement that the number N of multigroups is fixed, we shift multigroup boundaries, then we can decrease $[\delta\Sigma_g/\bar{\Sigma}_g]^2$ in one group only at the expense of increasing it in another. This can be expressed, at least qualitatively, by the requirement

$$\sum_g \langle [\delta\Sigma_g/\bar{\Sigma}_g]^2 \rangle = \text{constant} \quad . \tag{48}$$

The same comment applies to the sensitivity profile,

$$\sum_g P_g^2 = \text{constant.} \tag{49}$$

We note that both the flux and the adjoint flux peak in cross-section valleys and diminish in cross-section peaks (see analytic solution of Section V).

Moreover, the sensitivity profile contains both the group-integrated adjoint and flux, so it is roughly bilinear in the group width.

The minimum error in the integral nuclear design quantity (S^+,ψ) is obtained by minimizing Eq. (47) subject to Eqs. (48) and (49). The minimum occurs when both $\langle[\delta\Sigma_g/\Sigma_g]^2\rangle$ and P_g^2 are independent of group g, in accord with conditions A and B above, as was shown. Actually, as was noted above, our result is more general. The multigroup structure is to be chosen so as to minimize $\langle[\delta(S^+,\psi)]^2\rangle$ subject to the restriction that the number of groups is fixed at N. It may be that shifting group boundaries does not leave $\sum_g \langle[\delta\Sigma_g/\Sigma_g]^2\rangle$ constant or $\sum_g P_g^2$ constant. In this case, Eqs. (46) or (47) can be used to minimize $\sum_r w_r \langle[\delta(S_r^+,\psi)]^2\rangle$ by trial and error for a variety of integral responses r with weights w_r reflecting their importance to the nuclear design process.

VII. TECHNIQUE FOR SIMULTANEOUS ADJUSTMENT OF LARGE NUCLEAR DATA LIBRARIES (D. R. Harris and W. B. Wilson)

Successful nuclear design requires adequate prediction of integral design quantities such as critical loading, energy deposition rate, transmutation rate, Rossi-α, and radiation dose. Adequate prediction, in turn, requires an adequate nuclear data base, and a number of groups have attempted to achieve this by adjusting the data base to improve agreement with integral observations. These groups have in all practical cases utilized least square methods,[24] and whatever the functional to be minimized they have limited the adjustment to only a portion of a large nuclear data library. Had the adjustment been applied to another portion of the nuclear data library, another result would have been obtained. The limitation of adjustment to only a portion of the nuclear data library may be justified by physical intuition, but it also has been the result of technical problems in the required inversion of large matrices.[24] We show here that this inversion problem can be circumvented and arbitrarily large nuclear data libraries can be adjusted simultaneously when, as was assumed by most groups,[24] the basic nuclear data are uncorrelated. We illustrate the technique by adjusting nuclear data to integral observations (including very discrepant central worths) made on the ZPR-6-6A, ZPR-6-7, and ZPR-3-48 fast reactor benchmark critical assemblies.[25]

Group cross sections and other data in a nuclear data library will be represented by $x_1,x_2,\ldots,x_{\hat{j}}$, where $\hat{j}$, the number of primary parameters, may be of order 10^4 or 10^5. Integral parameters $y_1,y_2,\ldots,y_{\hat{i}}$ are computed as functions of the primary parameters, $y_i(x_1,x_2,\ldots,x_{\hat{j}})$, or $y_i(x)$ in a convenient notation. Here $\hat{i}$, the number of integral parameters usually is of order 10 to 10^2. From a combination of measurements, corrections, and calculations one arrives at "evaluated" observed values $x_1^e, x_2^e, \ldots, x_{\hat{j}}^e$, and $y_1^e, y_2^e, \ldots, y_{\hat{i}}^e$. It usually is found that $y_i(x^e)$ differs from y_i^e and we wish to reduce this discrepancy. One presumably can improve the data base by minimizing (other techniques are reviewed in Ref. 24),

$$S = \sum_{L=1}^{\hat{i}}\sum_{L'=1}^{\hat{i}} w_{y_i y_{i'}}[y_i(x) - y_i^e][y_{i'}(x) - y_{i'}^e]$$

$$+ \sum_{j=1}^{\hat{j}}\sum_{j'=1}^{\hat{j}} w_{x_j x_{j'}}[x_j - x_j^e][x_{j'} - x_{j'}^e]$$

$$+ 2\sum_{i=1}^{i}\sum_{j=1}^{i} x_j y_i [y_i(x) - y_i^e][x_j - x_j^e] \quad , \quad (50)$$

subject to the requirements that

$$y_i(x) = y_i(x^e) + \sum_{j=1}^{\hat{j}} \left.\frac{\partial y_i}{\partial x_j}\right|_{xe} [x_j - x_j^e] \quad , \quad (51)$$

$$i = 1,2,\ldots,\hat{i} \quad .$$

For minimum variances in the adjusted results, the weights w appearing in Eq. (50) are the elements of the inverse of the matrix of variances and covariances among the primary and secondary parameters. The use of a linear relation between y(x) and x in Eq. (51) results because the computation of $y_i(x)$ and $\delta y_i/\delta x_j$ (by perturbation theory) is obtained for the whole primary data base at once, not just a portion of it.

If we minimize S by obtaining $\hat{j}$ normal equations, then the combination of these and the $\hat{i}$ Eq. (51) represent i + j simultaneous equations. In general, the normal equations are solved by Gauss-Newton iteration;[26] here as in solution of the simutaneous linear Eqs. (50) and (51) large matrices, at least of order j x j, must be inverted. But if the primary parameters are uncorrelated with each other and with secondary parameters, the normal equations

$$\sum_{i=1}^{\hat{i}}\sum_{i'=1}^{\hat{i}} w_{y_i y_{i'}}[y_i(x) - y_i^e]\left.\frac{\partial y_{i'}}{\partial x_j}\right|_{x_e} + w_{x_j x_j}[x_j - x_j^e] = 0 \qquad (52)$$

$$j = 1,2,\ldots,\hat{j} \quad ,$$

permit the replacement of $x_j - x_j^e$ in Eq. (51) by linear combinations of $y_i(x) - y_i$. There result only $\hat{i}$ equations for $y_i(x) - y_i^e$

$$\sum_{i'=1}^{\hat{i}} [y_{i'}(x) - y_{i'}^e][\delta_{ii'} \times \left[\delta_{ii'} + \sum_{j=1}^{\hat{j}}\sum_{L''=1}^{\hat{L}} \frac{w_{L'L''}}{w_{x_j x_j}}\left.\frac{\partial y_{L''}}{\partial x_j}\right|_{x_e}\left.\frac{\partial y_i}{\partial x_j}\right|_{x_e}\right]$$

$$= y_L(x^e) - y_i^e \quad , \qquad (53)$$

$$L = 1,2,\ldots,\hat{L}$$

and, because $\hat{i}$ usually is much less than $\hat{j}$, the solution of Eq. (53) is a considerable computational improvement. Once the adjusted values $y_i(x)$ are computed from Eq. (53), the adjusted parameters are computed from Eq. (52) for the whole library at once. This adjustment technique has been coded as an option into the ALVIN sensitivity and adjustment code.

We illustrate this improved technique by adjusting nuclear data to $\hat{i} = 24$ integral observations on three ZPR assemblies described by Bohn.[25] Bohn supplies sensitivity coefficient information for only $\hat{j} = 19$ important primary nuclear data parameters so our technique is not really necessary (matrices or order $\hat{i} + \hat{j} = 43$ are readily inverted), but the principle at least is demonstrated. It is convenient to allow y_i to represent the ratio of the computed value C_i of an integral parameter to its experimental value of E_i, and to let x_j represent the ratio of the nuclear datum σ_j to its evaluated value σ_j^e; then y_i^e and x_j^e are unity, and

$$\left.\frac{\partial y_i}{\partial x_j}\right|_{xe} = \left.\left(\frac{\sigma_j}{C_i}\frac{\partial C_i}{\partial \sigma_j}\right)\right|_{xe} - \left.\left(\frac{\sigma_j}{E_i}\frac{\partial E_i}{\partial \sigma_j}\right)\right|_{xe} \quad . \qquad (54)$$

Specifically, for i = 1,2,3 the integral parameters are the C/E values for multiplication factors of ZPR-6-6A, ZPR-6-7, and ZPR-3-48, indicated in the second column of Table I by subscripts A, 7, and 8, respectively. For i = 4, 5, ..., 15 the integral parameters are the C/E values for central worths of ^{239}Pu, ^{235}U, ^{238}U, and ^{10}B, indicated by 49, 25, 28, and B, respectively, as superscripts on W; for example, the C/E value for the central worth of ^{239}Pu in the ZPR-6-7 assembly is indicated by W_7^{49} in Table I. Finally, for i greater than 15, the integral parameters y_i are C/E values of ratios of reaction rates, e.g., $_7R_{49f}^{28c}$ for y_{20} represents the C/E value of the ^{238}U capture rate relative to the ^{239}Pu fission rate measured in ZPR-6-7. If y_i is $(\sigma_n/\sigma_m)/(\sigma_n/\sigma_m)E$, then to first order (unchanged flux spectrum),

$$\left.\frac{\partial y_i}{\partial x_j}\right|_{xe} = \delta_{nj} - \delta_{mj} \quad . \qquad (55)$$

Primary nuclear data selected by Bohn for sensitivity studies are listed in Tables II and III together with sensitivity coefficients computed by Bohn and uncertainties assigned by Bohn. All Bohn's calculations utilize ENDF/B-III data as the evaluated base as processed into multigroup cross sections by SDX. All primary data were assumed to change independent of energy.

Values of primary and secondary parameters adjusted by ALVIN are listed in Tables I and III and show physically expected trends. Values selected by Bohn on the basis of the integral experiments also are listed. Our data adjustments are only illustrative of our adjustment technique. More detailed study of data uncertainties and sensitivities would be required to justify an adjusted data set for nuclear design application.

TABLE I

INTEGRAL PARAMETERS y_i and VALUES $y_i(x)^e$ COMPUTED USING EVALUATED NUCLEAR DATA PARAMETERS x_j^e

If no adjustment were necessary, $y_i(x^e)$ would equal unity

i	y_i	$y_i(x^e)$	y_i adjusted by ALVIN	y_i selected by Bohn
1	k_A	0.9920±0.004	0.992	
2	k_7	0.9924±0.004	1.002	
3	k_8	0.9927±0.004	1.002	
4	W_A^{49}	1.10 ±0.025	0.993	1.06
5	W_A^{25}	1.15 ±0.025	1.020	1.05
6	W_A^{28}	1.24 ±0.035	1.103	1.09
7	W_A^B	0.92 ±0.075	0.848	0.96
8	W_7^{49}	1.25 ±0.035	1.064	1.14
9	W_7^{25}	1.24 ±0.035	1.050	1.08
10	W_7^{28}	1.16 ±0.025	0.929	0.95
11	W_7^B	1.18 ±0.035	1.033	1.17
12	W_8^{49}	1.25 ±0.035	1.054	1.12
13	W_8^{25}	1.26 ±0.035	1.063	1.08
14	W_8^{28}	1.27 ±0.035	1.033	0.99
15	W_8^B	1.09 ±0.035	0.951	1.06
16	$_AR_{25f}^{28f}$	0.90 ±0.03	0.947	
17	$_AR_{25f}^{28c}$	1.03 ±0.03	1.063	
18	$_7R_{49f}^{28f}$	0.99 ±0.02	0.973	
19	$_7R_{49f}^{25f}$	1.05 ±0.02	1.033	
20	$_7R_{49f}^{28c}$	1.09 ±0.02	1.060	
21	$_7R_{25f}^{28f}$	0.94 ±0.02		
22	$_7R_{25f}^{28c}$	1.04 ±0.02	1.027	
23	$_8R_{25f}^{28f}$	0.96 ±0.05	0.960	
24	$_8R_{25f}^{28c}$	0.94 ±0.05	0.927	

VIII. MEDIUM ENERGY LIBRARY (D. G. Foster, Jr., W. B. Wilson, and D. R. Harris)

Monte-Carlo-history data sets for the basic NASA library have been completed. These were placed on the IBM Photostore device rather than on tape to improve the reliability of recovery. Since NASA plans to rely heavily on the isosinglet approximation to generate incident-neutron data from incident-proton calculations, all of the new histories are for incident protons at 15 energies (20, 25, 50, 100, 200, 300, 400, 500, 600, 700, 800, 1 000, 1 500, 2 500, and 3 500 MeV). Complete sets have been generated for the target nuclei ^{12}C and ^{16}O, in order to include explicit data on the heavy secondary charged particles for the elements which are most important in living tissue. Supplementary histories for incident protons at 20, 1 000, 1 500, 2 500, and 3 500 MeV have been generated for ^{27}Al and ^{56}Fe to fill out the existing sets already generated between 25 and 800 MeV.

A few additional changes in CROIX-2 have been found necessary. The most important of these are byproducts of the algorithm for salvaging intranuclear cascades which leave the residual nucleus with a negative excitation energy. When the overshoot is too drastic to salvage, or when the residual nucleus is impossible, the event is discarded and the event counter set back. Previously, CROIX-2 simply resumed with the next attempt. Now it discards any subsequent transparencies which occur, and resumes with the next reaction event (to replace the discarded reaction event), so as not to distort the ratio of reactions to transparencies. Data sets already generated before this error was discovered have been corrected by hand recalculation of the correct number of transparencies, using the diagnostic information printed out for each run.

In addition, the criterion for rejecting an energy overshoot has been weakened, since at energies below 400 MeV an excessive number of overshoots occurs which exceed 2% of the incident energy. The new criterion accepts overshoots up to 2% or 5 MeV, whichever is greater, up to an absolute maximum of 20% of the incident energy. For overshoot events which are accepted, the energies of emitted particles and of residual nucleus are scaled down so as to leave zero residual excitation energy. Instead of aborting the evaporation phase, however, these events are now submitted to the evaporation module to see whether evap-

TABLE II

SENSITIVITY COEFFICIENTS $(x_j/y_i)\partial y_i/\partial x_y$ for ZPR-6-6A, ZPR-6-7, and ZPR-3-48

```
 I  DYDX(I,J),J=1,MJ
 1  .61000E+00 -.10000E+00-0.          -0.          .80000E-01 -.27000E+00 -.30000E-01-0.          -0.          -0.
  -0.          -0.          -0.          -0.          -0.          -0.          -0.          -0.          -0.
 2-0.          -0.          .66000E+00 -.70000E-01  .80000E-01 -.26000E+00 -.60000E-01-0.          -0.          -0.
  -0.          -0.          -0.          -0.          -0.          -0.          -0.          -0.          -0.
 3-0.          -0.          .66000E+00 -.60000E-01  .90000E-01 -.21000E+00 -.70000E-01-0.          -0.          -0.
  -0.          -0.          -0.          -0.          -0.          -0.          -0.          -0.          -0.
 4 -.99100E+00  .49000E-01  .11600E+01 -.16100E+00 -.23900E+00 -.25500E+00  .47000E-01 -.45000E-01 -.11500E+00  .20000E-02
   -.60000E-02 -.30000E-02 -.14400E+00 -.85600E+00-0.          -0.          -0.          -.50000E-02-0.
 5  .26400E+00 -.17400E+00-0.          -0.          -.20600E+00  .21000E+00  .88000E-01 -.24000E-01 -.27000E-01  .10000E-01
    .20000E-02  .50000E-02 -.14400E+00 -.85600E+00-0.          -0.          -0.          .40000E-02-0.
 6 -.13450E+01 -.94000E-01-0.          -0.          -.58300E+00  .12250E+01  .34600E+00  .43000E-01  .14800E+00 -.14000E-01
    .20000E-02 -.20000E-02 -.14400E+00 -.85600E+00-0.          -0.          -0.          .20000E-02-0.
 7 -.12520E+01 -.14300E+00-0.          -0.          -.32900E+00 -.92000E-01  .20800E+00  .98000E-01  .21300E+00 -.20000E-01
    .40000E-02 -.30000E-02 -.14400E+00 -.85600E+00-0.          -0.          -0.          .20000E-02-0.
 8-0.          -0.           .21300E+00 -.83000E-01 -.41700E+00  .19900E+00  .11100E+00 -.27000E-01 -.52000E-01  .30000E-02
   -.30000E-02 -.20000E-02 -.32600E+00 -.25200E-01 -.59700E+00 -.20600E-01 -.31200E-01 -.10000E-02-0.
 9  .11790E+01 -.19000E+00 -.11010E+01  .50000E-01 -.39100E+00  .13700E+00  .15000E+00 -.40000E-02  .35000E-01  .90000E-02
    .30000E-02  .40000E-02 -.32600E+00 -.25200E-01 -.59700E+00 -.20600E-01 -.31200E-01  .60000E-02-0.
10-0.          -0.          -.12070E+01 -.12100E+00 -.77800E+00  .10450E+01  .49000E+00  .64000E-01  .19200E+00 -.20000E-01
    .30000E-02 -.30000E-02 -.32600E+00 -.25200E-01 -.59700E+00 -.20600E-01 -.31200E-01  .10000E-02-0.
11-0.          -0.          -.11290E+01 -.21600E+00 -.50900E+00 -.26000E+00  .28300E+00  .14900E+00  .31600E+00 -.33000E-01
    .40000E-02 -.40000E-02 -.32600E+00 -.25200E-01 -.59700E+00 -.20600E-01 -.31200E-01  .20000E-02-0.
12-0.          -0.           .24700E+00 -.69000E-01 -.46500E+00  .21100E+00  .14400E+00 -.90000E-02-0.           .10000E-02
   -.30000E-02 -.20000E-02 -.35600E+00 -.21000E-01 -.59900E+00 -.12100E-01 -.12100E-01 -.20000E-02 -.60000E-01
13  .11990E+01 -.21400E+00 -.10740E+01  .68000E-01 -.41700E+00  .16200E+00  .18300E+00 -.20000E-02-0.           .60000E-02
    .20000E-02  .30000E-02 -.35600E+00 -.21000E-01 -.59900E+00 -.12100E-01 -.12100E-01  .30000E-02  .57000E-01
14-0.          -0.          -.14460E+01 -.16700E+00 -.10260E+01  .12730E+01  .64000E+00  .47000E-01-0.          -.12000E-01
  -0.          -.40000E-02 -.35600E+00 -.21000E-01 -.59900E+00 -.12100E-01 -.12100E-01 -.10000E-02  .39500E+00
15-0.          -0.          -.11990E+01 -.27300E+00 -.56100E+00 -.22600E+00  .33800E+00  .85000E-01-0.          -.18000E-01
    .10000E-02 -.40000E-02 -.35600E+00 -.21000E-01 -.59900E+00 -.12100E-01 -.12100E-01-0.           .51700E+00
16 0.          -.10000E+01 0.          0.          0.           .10000E+01 0.          0.          0.          0.
   0.          0.          0.          0.          0.          0.          0.          0.          0.
17 0.          -.10000E+01 0.          0.           .10000E+01 0.          0.          0.          0.          0.
   0.          0.          0.          0.          0.          0.          0.          0.          0.
18 0.          0.          -.10000E+01 0.          0.           .10000E+01 0.          0.          0.          0.
   0.          0.          0.          0.          0.          0.          0.          0.          0.
19  .10000E+01 0.          -.10000E+01 0.          0.          0.          0.          0.          0.          0.
   0.          0.          0.          0.          0.          0.          0.          0.          0.
20 0.          0.          -.10000E+01 0.           .10000E+01 0.          0.          0.          0.          0.
   0.          0.          0.          0.          0.          0.          0.          0.          0.
21 -.10000E+01 0.          0.          0.           .10000E+01 0.          0.          0.          0.          0.
   0.          0.          0.          0.          0.          0.          0.          0.          0.
22 -.10000E+01 0.          0.          0.           .10000E+01 0.          0.          0.          0.          0.
   0.          0.          0.          0.          0.          0.          0.          0.          0.
23 -.10000E+01 0.          0.          0.          0.           .10000E+01 0.          0.          0.          0.
   0.          0.          0.          0.          0.          0.          0.          0.          0.
24 -.10000E+01 0.          0.          0.           .10000E+01 0.          0.          0.          0.          0.
   0.          0.          0.          0.          0.          0.          0.          0.          0.
```

TABLE III

PRIMARY NUCLEAR DATA PARAMETERS x_j, THEIR UNCERTAINTIES, AND THEIR ADJUSTED VALUES

j	x_j	x_j^e	x_j adjusted by ALVIN	x_j selected by Bohn
1	σ_f^{25}	1±0.1	0.971	0.93
2	σ_c^{25}	1±0.1	0.925	
3	σ_f^{49}	1±0.1	0.983	0.97
4	σ_c^{49}	1±0.1	0.994	
5	σ_c^{28}	1±0.15	0.953	0.88
6	σ_f^{28}	1±0.1	0.971	0.97
7	σ_{inel}^{28}	1±0.15	0.793	0.88
8	σ_{el}^{Na}	1±0.1	1.063	
9	σ_{el}^{O}	1±0.1	1.075	
10	σ_c^{Fe}	1±0.1	0.977	
11	σ_c^{Ni}	1±0.1	1.001	
12	σ_c^{Cr}	1±0.1	0.995	
13	$\bar{\nu}_d^{28}$	1±0.06	1.153	1.10
14	$\bar{\nu}_d^{25}$	1±0.04	1.109	1.012
15	$\bar{\nu}_d^{49}$	1±0.06	1.190	1.024
16	$\bar{\nu}_d^{40}$	1±0.1	1.011	1.016
17	$\bar{\nu}_d^{41}$	1±0.1	1.012	
18	σ_c^{Na}	1±0.1	0.995	
19	σ_{el}^{C}	1±0.1	1.097	

oration can occur. This allows unstable residual nuclei from the cascade phase, notably ^{8}Be, to disintegrate spontaneously as they should. The Wapstra mass table was arbitrarily altered (within experimental uncertainty) so as to insure that ^{5}H will decay into ^{4}H under this circumstance. This provision often leads to the emission of several evaporated particles, thus restoring some of the emitted-particle energy removed in the scaling process.

In an effort to simplify post-processing of the history data sets, a second file has been added to the output to record the total number of transparencies and reactions contained in the set (the transparencies are omitted from the detailed histories). In addition, a complete record of the input conditions is appended to the first event in each data set.

The first-generation processor for converting the Monte Carlo histories into cross-section input for NASA's applications is nearly ready for production use. Christened NASPRO, it is related to the code DANAl used to produce DTF-format output from these histories in the past. In its present form, the main information compiled from the histories is a table of Legendre coefficients which describe the angular distributions of secondary nucleons and mesons in each of up to 452 energy bins. By summing this array over all energies, gross angular distributions can be reproduced. These are integrated analytically in an iterative search for equiprobability boundaries for the overall angular distributions. Using these production-cosine boundaries, integrals in each of the 452 energy groups are then used to determine the boundaries of 40 equally probable energy bins within each of 10 equally probable cosine bins. For nucleons this is done for energies above 20 MeV; for mesons it extends over all observed energies. Nucleons below 20 MeV are assumed isotropic and binned into 20 equally probable energy intervals. The original 452 energy groups are adjusted so as to give accurate linear interpolation in energy for each secondary particle type at every energy. Multiplicities, average energies, average production cosines, the nonelastic cross section, and other useful quantities are included in the output.

The adequacy of the Legendre-expansion approach is currently being investigated in detail. Because secondary particles produced at energies near the primary energy cannot reach all angles, the distributions in this energy region have sharp cutoffs in cosine which produce pathological Legendre expansions. It is clear from a test analysis for 800-MeV protons on ^{16}O that 20 coefficients are not sufficient, since the actual number of events in supposedly equally probable bins is wrong by as much as a factor of 2 in a few instances. If the addition

of a reasonable number of coefficients fails to solve this problem, it will be necessary to use some kind of a priori cosine-bin structure.

IX. ENDF/B-IV YIELD, DECAY, AND CROSS-SECTION FILES (T. R. England, N. L. Whittemore)

A. Yields

The final sets of ENDF/B-IV direct nuclide yields per fission were completed in a cooperative LASL, HEDL, and GE effort. Various weighted yield quantities were computed after revising a local processing code. Similar quantities were also computed at GE, HEDL, and CRNL and the results transmitted to appropriate CSEWG groups.

Some yield weighted quantities and delayed neutron yields per fission were computed because of their immediate utility in locating yield sets most in need of data, and possibly in improving the current yield distribution model.

The yield processing code was further modified to process ENDF yields into a new CINDER format. This will be used at LASL; a copy was sent to the Bettis Atomic Power Laboratory for use in a revised version of CINDER. This tape contains both independent and cumulative nuclide yields.

Some current coding effort is directed at producing readable listings of the 11,313 final independent ENDF/B-IV yields for use in a joint LASL/HEDL report.

B. Activation Cross Sections

The ENDF/B-IV decay/absorption files do not contain activation cross sections. A preliminary listing of values for the 181 nuclides having capture cross sections in these ENDF/B-IV files was compiled and distributed for comment within the decay/absorption data task force. Activation cross sections are essential for use in nuclide transmutation computations, and LASL/ORNL/HEDL agreement is needed for the anticipated comparison computations of decay heating.

C. Nuclide Chains

The complex nuclide chain structure showing all neutron couplings and decay branching for the 824 fission product nuclides in ENDF/B-IV has been completed. This will be used to generate the linear chains needed in nuclide computations. Some chain data are still preliminary, but final data are complete for 400 nuclides and the remainder should be available during the first month of the next quarter.

Preliminary data are available for all nuclides; a code was written to process the primary decay and absorption parameters into a compact, readable listing and distributed to interested groups within LASL and a copy was sent to DNA and DRRD.

X. ABSORPTION LIBRARY FOR FISSION PRODUCTS (T. R. England and N. L. Whittemore)

A chain library consisting of all decay cross section and yield parameters needed in estimating neutron absorption buildup in the fission of ^{233}U, ^{235}U, ^{238}U, ^{239}Pu, and ^{232}Th was prepared. This library is in the new CINDER-7 format. It was prepared following a request for survey studies of nuclides generated during irradiation of a CTR blanket of fertile material. It will be useful in other studies such as HTGR safety. This library does not contain short lived (<5 h) nuclides and therefore is not intended for use in decay heat estimates.

XI. GAS CONTENT IN IRRADIATED FUELS (T. R. England)

Following a request from AEC Regulatory, tables of the buildup and decay of fission product gas for several fuels, irradiation and cooling intervals were prepared using the new absorption library. These data were needed by the AEC to assist Regulatory in supplying answers to queries by the GAO. Copies of these data were also supplied to DRRD.

XII. CINDER CODE (T. R. England and N. L. Whittemore)

CINDER-7, having the features described in the last two progess reports, has been further extended and many validation calculations were completed during this quarter. This improved code is available for LASL users.

Cooperation with the Bettis (Westinghouse) and Knolls (GE) Atomic Power Laboratories continues in further major revisions to retain the improved features while eliminating redundant I/O and storage. This version is more appropriate for the mass of ENDF/B-IV data and will be useful in a wider range of applications.

XIII. GAMMA AND PHOTONEUTRON SPECTRA (T. R. England, M. G. Stamatelatos, and N. L. Whittemore)

ENDF/B-IV contains ten sets of nuclide yields for six fuels. These and decay data were incorporated into a CINDER-7 library and gamma spectra computed

for all ten sets for use in a new code, PHONEX. Preliminary $^{2}H(\gamma,n)$ calculations of neutron spectra were completed near the end of this quarter and $^{9}Be(\gamma,n)$ spectra will be completed during the early part of the next quarter. An extensive report on these spectra, the general PHONEX code and an article are in preparation. Typical results will be reported in the next quarter and presented at the March 1975 APS Conference on Nuclear Cross Sections and Technology in Washington, D. C.[27]

XIV. STUDY OF THE $T(d,n)^{4}He$ CROSS SECTIONS (G. M. Hale and L. Stewart)

The $T(d,n)^{4}He$ reaction is perhaps the most important, and presumably the best-determined, of all the fusion reactions. Most measurements of the integrated cross section are nearly 20 years old, however, and considerable uncertainty occurs in extrapolating the low energy measurements to zero energy.

We have checked many of the T(d,n) measurements by including them in a preliminary, but comprehensive R-matrix analysis of reactions in the five-nucleon system at low energies. This analysis, originated by Nisley, Hale, and Dodder, includes data from the reactions T(d,d)T, $T(d,n)^{4}He$, and $^{4}He(n,n)^{4}He$ in the ^{5}He system, as well as data from the reactions $^{3}He(d,d)^{3}He$, $^{3}He(d,p)^{4}He$, and $^{4}He(p,p)^{4}He$ in the ^{5}Li system. These data include, in addition to the integrated reaction cross sections, differential cross sections, polarizations, and analyzing tensors for the deuteron-induced reactions. Resonance parameters in the two system (^{5}He and ^{5}Li) are related by charge symmetry, so that all the reactions are analyzed simultaneously.

A satisfactory fit to all the data included in the analysis has been obtained. The calculated T(d,n) integrated cross section appears to follow the measurements of Conner et al.[28] at energies between 15 and 600 keV, but lies systematically above Conner's points outside the interval. Examination of the calculated cross section at low energies reveals that deviations from the Gamow form (the cross section descends more steeply with decreasing energy than does the Gamow form) persist down to energies as low as 2 keV. These deviations are attributed to the energy dependence of terms describing the broad 3/2+ resonance at $E_d \approx 107$ keV. The calculated cross sections below 20 keV agree surprisingly well with measurements of Arnold et al.[29] although the authors discounted their own measurements and relied on a Gamow extrapolation to provide low-energy points in a later publication.[30]

This information has been included in a report[15] prepared during this quarter, discussing the status of measurements and parameterizations for two of the important fission reactions, $T(d,n)^{4}He$ and $T(t,2n)^{4}He$ at energies below 1 MeV.

XV. NEUTRON-INDUCED GAMMA-RAY PRODUCTION CROSS SECTIONS FOR TUNGSTEN (P. G. Young)

A report[31] has been written describing evaluations of neutron-induced gamma-ray production cross sections for ^{182}W, ^{183}W, ^{184}W, and ^{186}W that were adopted for Version IV of ENDF/B. The evaluations for energies in the keV region are based on calculations and in the thermal and MeV regions on experimental data for natural tungsten that have been fitted with a simple statistical theory. The theory was used to facilitate smoothing and extrapolation to unmeasured neutron and gamma-ray energies, and to derive the constituent ^{182}W, ^{183}W, ^{184}W, and ^{186}W data from the natural element measurements, so that the isotopic data could be combined with evaluations of neutron-production cross sections performed elsewhere.

XVI. A NEW n-d EVALUATION FOR DNA (L. Stewart and R. J. LaBauve)

The n-d evaluation performed by Horsley (AWRE) and Stewart (LASL) was placed in the ENDF/B format at the request of the Defense Nuclear Agency (DNA). Before this evaluation (Anthony Horsley and Leona Stewart, "Evaluated Neutron Cross Sections for Deuterium," LA-3271 [1968]) was submitted to RSIC, corrections were made to the low-energy cross sections and gamma production data were added. It is now part of the DNA library.

XVII. PROPOSED FORMAT FOR NEUTRON-INDUCED RADIOACTIVE DECAY DATA IN ENDF/B (L. Stewart, R. J. LaBauve, and P. G. Young)

A format description for providing neutron-induced radioactive decay data in the ENDF/B files was proposed and distributed. This proposal is being pursued in concert with the CSEWG Subcommittee on Radioactive Decay Data at the request of the United States Nuclear Data Committee CTR Subcommit-

tee. At the present time, DNA and DMA have also expressed interest in such data and both organizations would like to have a format proposed and adopted for the ENDF system.

XVIII. EVALUATIONS OF NEUTRON-INDUCED CROSS SECTIONS OF Li AND ^{15}N (P. G. Young, L. Stewart, G. M. Hale, E. D. Arthur, and D. M. McClellan)

We have assembled the relevant published literature and experimental data in preparation for evaluations of the neutron-induced cross sections of ^{6}Li and ^{15}N.

The ^{6}Li evaluation will cover the range 1-20 MeV and will be an extension of our earlier analysis at lower energies that was incorporated into Version IV of ENDF/B. Our primary goal is to revise the $^{6}Li(n,n'd)\alpha$ cross sections to more accurately represent experimental data and to include energy-angle correlations between secondary neutrons. The latter task will be accomplished by using a discrete level representation with fictitious levels included where necessary to describe the secondary neutron spectrum thus obviating the need for the more cumbersome File 6 representation in ENDF/B. Revisions to the elastic cross section and angular distributions are also planned, where indicated.

The ^{15}N evaluation will cover the energy range from 10^{-5} eV to 20 MeV. We are presently examining the available level parameter assignments for ^{16}N in preparation for an R-matrix analysis with the fitting code EDA. We plan to adopt the resonance parameters obtained by Zeinitz et al.,[32] and to refine and extend that analysis to higher energies, as time permits.

REFERENCES

1. B. M. Carmichael, "Standard Interface Files and Procedures for Reactor Physics Codes, Version III," Los Alamos Scientific Laboratory report LA-5486-MS (1974).

2. R. E. Schenter, J. L. Baker, and R. B. Kidman, "ETOX, A Code to Calculate Group Constants for Nuclear Reactor Calculations," Battelle Northwest Laboratory report BNWL-1002 (1969).

3. R. W. Hardie and W. W. Little, Jr., "1DX, A One-Dimensional Diffusion Code for Generating Effective Nuclear Cross Sections," Battelle Northwest Laboratory report BNWL-954 (1969).

4. R. J. LaBauve, C. R. Weisbin, R. E. Seamon, M. E. Battat, D. R. Harris, P. G. Young, and M. M. Klein, "PENDF: A Library of Nuclear Data for Monte Carlo Calculations Derived from Data in the ENDF/B Format," Los Alamos Scientific Laboratory report LA-5687 (1974).

5. C. R. Weisbin and R. J. LaBauve, "Specification of a Generally Useful Multigroup Structure for Neutron Transport," Los Alamos Scientific Laboratory report LA-5277-MS (1973).

6. D. E. Cullen, "Program SIGMA1 (Version 74-1)," Lawrence Livermore Laboratory report UCID-16426 (January 1974).

7. C. R. Weisbin, P. D. Soran, and J. S. Hendricks, "A New Procedure for the Determination of Neutron Multigroup Transfer Matrices," Nucl. Sci. Eng. 55, 329 (1974).

8. C. R. Weisbin, P. D. Soran, D. R. Harris, R. J. LaBauve, and J. S. Hendricks, "MINX -- A Multigroup Interpretation of Nuclear X-Sections," Trans. Am. Nucl. Soc. 16, 127 (1973).

9. Y. D. Naliboff and J. U. Koppel, "HEXSCAT, Coherent Elastic Scattering of Neutrons by Hexagonal Lattices," GA-6026 (1964).

10. W. W. Clendenin, "Calculation of Thermal Neutron Scattering Cross Section for Crystalline Materials: The TOR Program," Los Alamos Scientific Laboratory report LA-3823 (1967).

11. H. C. Honeck and D. R. Finch, "FLANGE-II (Version 71-1), A Code to Process Thermal Neutron Data from an ENDF/B Tape," E. I. DuPont de Nemours & Company Savannah River Laboratory report DP-1278 (1971).

12. W. W. Clendenin, "Calculation of Thermal Neutron Diffusion Length and Group Cross Sections: The GLEN Program," Los Alamos Scientific Laboratory report LA-3893 (1968).

13. K. D. Lathrop, "DTF-IV, A Fortran-IV Program for Solving the Multigroup Transport Equation with Anisotropic Scattering," Los Alamos Scientific Laboratory report LA-3373 (1965).

14. R. J. LaBauve, private communication.

15. Leona Stewart and Gerald M. Hale, "The $T(d,n)^{4}He$ and $T(t,2n)^{4}He$ Cross Sections at Low Energies," Los Alamos Scientific Laboratory report LA-5828-MS and USNDC-CTR-2 (1974).

16. D. R. Harris, P. G. Young, and G. M. Hale, "Characterization of Uncertainties in Evaluated Cross Section Sets," Trans. Am. Nucl. Soc. 16, 323 (1973).

17. S. A. W. Gerstl, D. J. Dudziak, and D. W. Muir, "A Quantitative Assessment of CTR Nuclear Data Needs," to be published in the Proc. of the Conf. on Nuclear Cross Sections and Tech., Washington, D. C. (1975).

18. G. M. Hale, D. R. Harris, and R. E. MacFarlane, "Applied Nuclear Data Research and Development Quarterly Progress Report, July 1 through September 30, 1974," Los Alamos Scientific Laboratory report LA-5804-PR (1974).

19. Ibid, p. 1.

20. G. M. Hale, D. R. Harris, and R. E. MacFarlane, "Applied Nuclear Data Research and Development Quarterly Progress Report, January 1 through March 31, 1974," Los Alamos Scientific Laboratory report LA-5655-PR (1974).

21. D. E. Bartine, F. R. Mynatt, and E. M. Oblow, "SWANLAKE, A Computer Code Utilizing ANISN Radiation Transport Calculations for Cross Section Sensitivity Analysis," Oak Ridge National Laboratory report ORNL-TM-3809 (1973).

22. D. E. Bartine, E. Oblow, and F. R. Mynatt, "Sensitivity Analysis: A General Approach Illustrated for a Na-Fe System," Proc. National Topical Meeting on New Development in Reactor Physics and Shielding, Kiamesha Lake, CONF-720901, Book 1 (1972) p. 5.

23. E. Oblow, J. Ching, and J. Drischler, "Selection of Group Energy Boundaries Using Sensitivity Theory," Trans. Am. Nucl. Soc. 17, 547 (1973).

24. D. R. Harris, "Consistency Among Differential Nuclear Data and Integral Observations," Trans. Am. Nucl. Soc. 18, 340 (1974).

25. E. M. Bohn, "The Central Worth Discrepancy in Three Fast Reactor Benchmark Critical Assemblies," Argonne National Laboratory report ZPR-TM-185 (1974).

26. D. R. Harris, "DAFT1 -- A FORTRAN Program for Least Square Fitting of 0.0253 eV Neutron Data for Fissile Nuclides," Westinghouse Electric Corporation report WAPD-TM-761 (1968).

27. M. G. Stamatelatos and T. R. England, "Fission-Product Gamma-Ray and Photoneutron Spectra," to be published in the Proc. of the Conf. on Nuclear Cross Sections and Tech., Washington, D. C. (1975).

28. J. P. Conner, T. W. Bonner, and J. R. Smith, "A Study of the $^{3}H(d,n)^{4}He$ Reaction," Phys. Rev. 88, 468 (1952).

29. W. R. Arnold, J. H. Phillips, G. H. Sawyer, E. J. Stovall, and J. L. Tuck, "Absolute Cross Section for the Reaction $T(d,n)^{4}He$ from 10 to 120 keV," Los Alamos Scientific Laboratory report LA-1479 (1953).

30. W. R. Arnold, J. A. Phillips, G. H. Sawyer, E. J. Stovall, and J. L. Tuck, "Cross Sections for the Reactions $D(d,p)T$, $D(d,n)^{3}He$, $T(d,n)^{3}He$, and $^{3}He(d,p)^{4}He$ Below 120 keV," Phys. Rev. 93, 483 (1954).

31. P. G. Young, "An Evaluation of Gamma Ray Production Cross Sections from Neutron-Induced Reactions on Tungsten," Los Alamos Scientific Laboratory report LA-5793, to be published (1975).

32. B. Zeitnitz, H. Dubenkropp, R. Putzki, G. J. Kirouac, S. Cierjacks, J. Nebe, and C. C. Dover, "Neutron Scattering from ^{15}N," Nuc. Phys. A166, 443 (1971).